A design optimization method for solar-driven thermochemical storage systems based on building performance simulation

Journal of Energy Storage 72 (2023) 108354

Contents lists available at ScienceDirect

Journal of Energy Storage

journal homepage: www.elsevier.com/locate/est

Research papers

A design optimization method for solar-driven thermochemical storage systems based on building performance simulation

Shuwei Wang [a,*], Pieter-Jan Hoes [a], Jan L.M. Hensen [a], Olaf C.G. Adan [b,c,d], Pim A.J. Donkers [d]

[a] Department of the Built Environment, Eindhoven University of Technology, Eindhoven, the Netherlands
[b] Department of Applied Physics, Eindhoven University of Technology, Eindhoven, the Netherlands
[c] TNO Materials Solutions, Eindhoven, the Netherlands
[d] Cellcius B.V., Eindhoven, the Netherlands

ARTICLE INFO

Keywords:
Thermochemical heat storage
Building performance simulation
Solar energy
Simulation-based optimization
Surrogate model

ABSTRACT

The challenge of the temporal mismatch between energy supply and demand in buildings is growing with the increasing share of renewable energy in total energy consumption. Among all the state-of-the-art energy storage solutions, thermochemical heat storage shows a unique potential thanks to its considerable energy density, acceptable cost, and negligible heat loss. For this reason, it becomes a promising alternative to common sensible heat storage solutions for building applications. The integration of such a novel technology in buildings necessitates a method for the assessment of its potential impact and benefit, the comparison to common alternatives, and the optimization of the system design. This work proposes a method based on modeling and simulation of the interaction between the thermochemical heat storage system and the building using a data-driven surrogate model of the storage system in combination with a building performance simulation engine. The data-driven model was developed and validated based on laboratory measurements of a novel closed-loop thermochemical heat storage system, the heat battery (HB). The method was demonstrated in a case study to identify the optimal size of the HB in a solar-driven configuration based on a residential building use case. The results show that the heat battery can digest the thermal energy transferred from the solar thermal collector to reduce the original electricity consumption for heating the detached house (0.7 MWh to 1.0 MWh in considered cases) without any obvious sacrifice in thermal comfort and that the small-scale HB (with a storage volume below 160 l) shows efficient usage of the designed storage capacity.

1. Introduction

As the largest energy-consuming sector in the world, buildings account for one-third of the total final energy consumption and represent an equally significant source of carbon dioxide (CO_2) emissions [1]. For buildings in European Union, around 70 % of energy is consumed for heating, cooling, and hot water production [1]. To reduce CO_2 emissions from this part, various strategies have been implemented including the promotion of renewable energy sources. In the European Union, the share of renewable energy in gross final energy consumption for heating and cooling has increased from approximately 12 % in 2005 to over 23 % in 2020 [2]. This growth in renewable energy share is raising the challenge of the mismatch between energy supply (heat or electricity) and building demand. One promising strategy toward this challenge is to use energy storage technologies to decouple the generation and consumption of energy (heat or electricity) [3,4] and enhance the flexibility of the entire system [5].

Various energy storage technologies are applied in buildings, such as electrical batteries [6,7], water tanks [8,9], phase change materials (PCMs) [10,11], buildings thermal capacitance [12], and thermochemical storage materials (TCMs) [13,14]. While electrical batteries have the advantage of high year-round utilization because of the constant presence of electric loads in buildings, thermal energy storage technologies (water tanks, PCMs, and TCMs) are more cost-effective in many situations due to their lower capital cost and longer lifetime [15–17]. A typical use case of thermal energy storage technologies in buildings is to use them to digest on-site solar thermal energy [18–20], while sensible heat storage technologies, like water tanks, are the most widely used at present [13], thermochemical heat storage systems possess a superior potential due to their high energy density (approximately 1GJ/m^3 [21–23]) and negligible heat loss. However, commercial

* Corresponding author at: P.O. Box 513, 5600 MB Eindhoven, the Netherlands.
E-mail address: s.wang5@tue.nl (S. Wang).

https://doi.org/10.1016/j.est.2023.108354
Received 12 January 2023; Received in revised form 2 June 2023; Accepted 9 July 2023
Available online 17 July 2023

Nomenclature

Abbreviations

ANN	Artificial neural network
API	Application programming interface
BPS	Building performance simulation
CV(RMSE)	Coefficient of variation of the root mean square error
HB	Heat battery
HVAC	Heating, ventilation, and air-conditioning
MAPE	Mean average percentage error
PCM	Phase change material
RMSE	Rooted mean square error
TCM	Thermochemical storage material
WT	Water tank

Symbols

COP_c	coefficient of performance for charging the HB
COP_d	coefficient of performance for discharging the HB
e_c	electric power for driving the charging cycle, kW
e_d	electric power for driving the discharging cycle, kW
m_c	charging fluid mass flow rate, kg/s
m_d	discharging fluid mass flow rate, kg/s
q_c	actual thermal power charged into the TCMs, kW
$q_{c\text{-}t}$	target thermal charging power of the HB, kW
q_d	actual thermal power discharged from the TCMs, kW
$q_{d\text{-}t}$	target thermal discharging power of the HB, kW
$t_{c\text{-}in}$	charging fluid temperature at the heat exchanger inlet, °C
$t_{c\text{-}out}$	charging fluid temperature at the heat exchanger outlet, °C
$t_{d\text{-}in}$	discharging fluid temperature at the heat exchanger inlet, °C
$t_{d\text{-}out}$	discharging fluid temperature at the heat exchanger outlet, °C
η_c	thermal efficiency of charging the HB
η_d	thermal efficiency of discharging the HB

thermochemical heat storage solutions are not available yet, and the current prototypes [24–26] still have some limitations concerning the volume of the required system components and the required energy for driving the system [13]. Before large-scale commercialization of thermochemical heat storage technologies in buildings can happen, it is crucial to understand the most promising use cases of the technology [27]. In order to identify the potential of a use case it is necessary to assess the impact of the technology on the performance of buildings while optimizing the system design and considering the perspectives of various stakeholders.

One research approach is to test the thermochemical heat storage system in buildings through simulation experiments, but there is still a knowledge gap in the methodology for the dynamic simulation of TCM system models with effective building models. An existing approach is to derive the storage system model from some physical principles such as isothermal energy balance, then integrate it with some simplified building or heat demand models [28–30]. This type of approach enables the virtual test of different TCM system configurations but can hardly achieve a fit-for-purpose model complexity of buildings. From this perspective, building performance simulation (BPS) can provide a more complete virtual building testbed [31]. BPS considers the dynamic interactions between the geometry and thermal properties of a building, energy systems, occupant behaviors, and climate conditions [32], and thus provides a valuable virtual building test environment for supporting the decision-making in the R&D phase of such innovative building technologies. Nonetheless, although existing modeling techniques for thermochemical storage already cover various scales from molecular level [33], grain level [34], powdery level [35], reactor level [36], and even system-level [28], current BPS tools still have no models which are directly usable. The implementation of the aforementioned modeling techniques in BPS remains challenging due to their high cost of computation caused by the high model complexity [37]. Therefore, some researchers chose to export the heat demand profiles from a BPS tool and model the storage system separately [38]. This approach would ignore the dynamic interaction between the buildings, occupants, and the TCM systems, and thus could not reflect the full impact that the TCM system might have on some aspects of building performance (such as indoor thermal comfort). Hence, there is a need for an effective modeling and simulation approach for thermochemical heat storage systems in BPS tools. This study fills this gap and establishes a virtual building testbed for a state-of-the-art closed-loop thermochemical heat storage system, the heat battery (HB). It is conducted in cooperation with the HB developers and aims to deliver both valuable suggestions for HB's design optimization and solutions to the knowledge gap mentioned above.

The main contribution of this article is the novel simulation-based methodology that enables the assessment and optimization of a solar-driven thermochemical storage system applied to a renovated dwelling with an air-source heat pump. The system design is assessed and optimized based on the dwelling's performance in various scenarios. A surrogate model of the heat battery is developed and validated based on a dataset from earlier research. This model is implemented in the EnergyPlus simulation program via a novel plugin written in Python, in combination with a building model developed and validated based on previous studies and literature information [27,39–42]. The implementation of the models was verified by analyzing the results from a test simulation run. In the weather conditions of Eindhoven and Marseille, 14 variants of the solar-driven heat battery system were tested and compared to equal-storage-volume water tank systems. The core focus of this paper is on the method for assessing application potential and optimizing capacity design toward building integration. This research aims to evaluate the feasibility, benefits, and comparison of solar-driven thermochemical storage systems with conventional alternatives. The proposed methodology integrates building performance simulation and a data-driven surrogate model, enabling the optimization of system design based on specific building requirements and characteristics. The following parts of this article are structured as: Section 2 introduces the methodology that is proposed and employed by this study. Section 3 presents the detailed simulation results of the verification study and the design optimization cases. Section 4 discusses the contribution and limitations of this work and concludes the whole article with the diverse potential of the HB.

2. The proposed method

The method used in this research consists of three major parts. Part I is the development and validation of the surrogate HB model. Part II is the implementation of the developed HB model in BPS and the verification of this implementation. Part III is the design optimization of the system in a defined use case of the HB. Fig. 1 provides an overview of the proposed method.

2.1. Part I – HB model development and validation

2.1.1. System investigation

The prototype of the heat battery uses the reversible hydration mechanism of a type of TCM – potassium carbonate (K_2CO_3). As shown in Fig. 2, it contains a storage module (on the right of the picture) for the

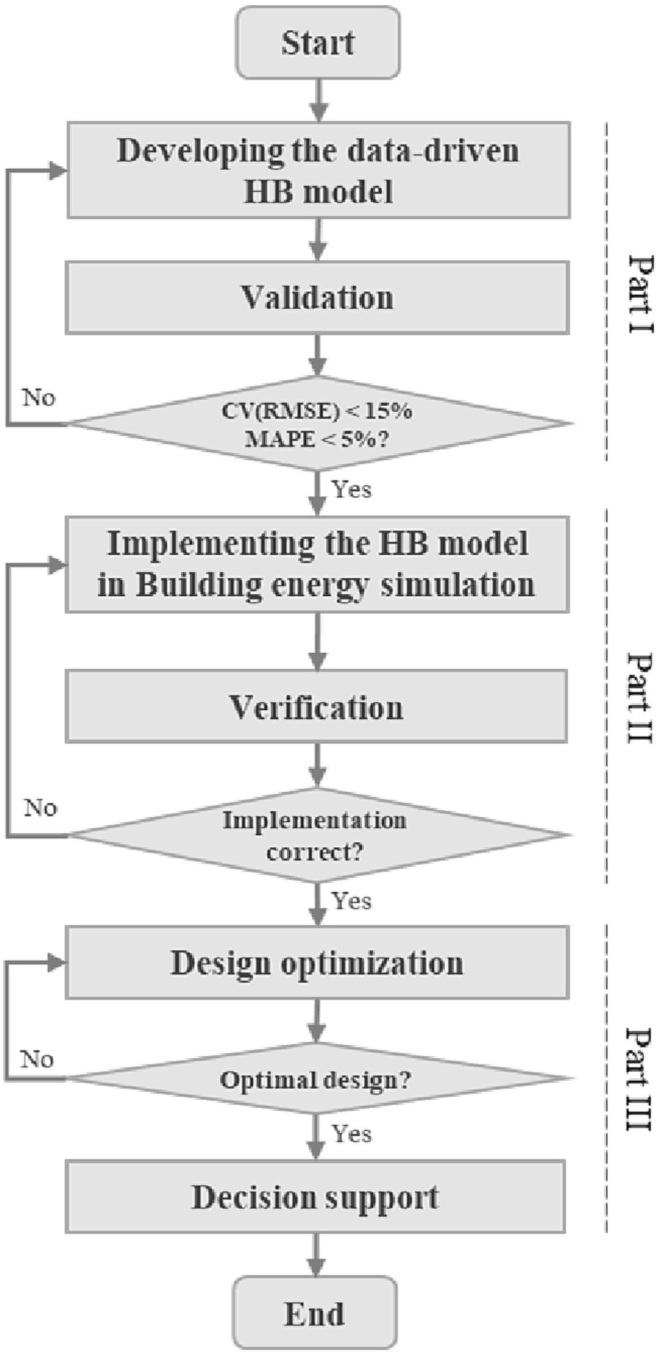

Fig. 1. Flowchart of the research methodology.

composites and an electricity-driven mechanical system (on the left of the picture) to maintain continuous charging or discharging powers. The developers have taken some measures for accelerating the reaction kinetics as described in previous literature [44]. Because the discharging power is directly related to the amount of thermochemical material, the discharging power can also be scaled based on specific application requirements.

To start charging or discharging the heat battery, the building energy system first needs to set a target power for charging or discharging. According to this target, the heat battery adjusts the powers of the fan, the pump, and other components and starts to intake the fluid in the heat exchangers. After the charging or discharging process completes, these components will be turned off to switch the heat battery into standby mode when its heat loss is negligible.

Fig. 2. The prototype of the heat battery [43].

The charging model of the heat battery takes the inlet temperature and mass flow rate of the charging fluid and the target charging power as input variables, as Fig. 3 illustrates. It calculates the outlet temperature of the corresponding fluid, the actual charging power, and the electric power as output variables. The discharging model uses a similar set of input and output variables.

2.1.2. *Selecting modeling method*

Based on prior experimental findings, the developer has recognized the need for a high-resolution model of the HB, as its transient performance is likely to be significantly influenced by various input factors, including but not limited to the temperature of the fluid during charging and discharging processes in the associated buildings. Therefore, the developer of the HB has constructed a high-resolution model based on the physical principles and laboratory experiments and has programmed it into a MATLAB program. This model can predict the transient values of some state variables based on several input values and detailed design parameters such as porosity, grain diameter, the dimension of the TCM module, heat exchanger effectiveness, and the air pressure range. This model has been validated to predict HB's performance, but it is relatively computationally expensive compared to common BPS tools such as EnergyPlus. For instance, it takes around 1 min to calculate one group of output variables for charging the HB, but just 50 s to complete a whole-year simulation of a detached house in EnergyPlus (with a 15-min timestep on the same computer). If the high-resolution HB model is directly implemented in the simulation tool, the number of desired virtual tests will be limited by the computational time.

A possible solution is to construct a surrogate model of the high-resolution model. A dataset is already available for training a surrogate model based on previous lab experiments and the high-resolution model. It has thousands of observations for both the charging process (over 21,000 observations) and discharging process (over 391,000 observations) and covers a wide range of values of the input variables and output variables shown in Fig. 3. This provides us with the possibility of developing data-driven models that can be both accurate enough and computationally cheap.

2.1.3. *Model training and validation*

To train a surrogate model based on the dataset, an algorithm is needed to predict the numerical values of multiple output variables based on multiple numerical inputs. Because the inputs and outputs are known in the dataset, the algorithm should be a supervised learning one such as a neural network. In the supervised neural network, the predicted outputs of the network are compared with the actual outputs in

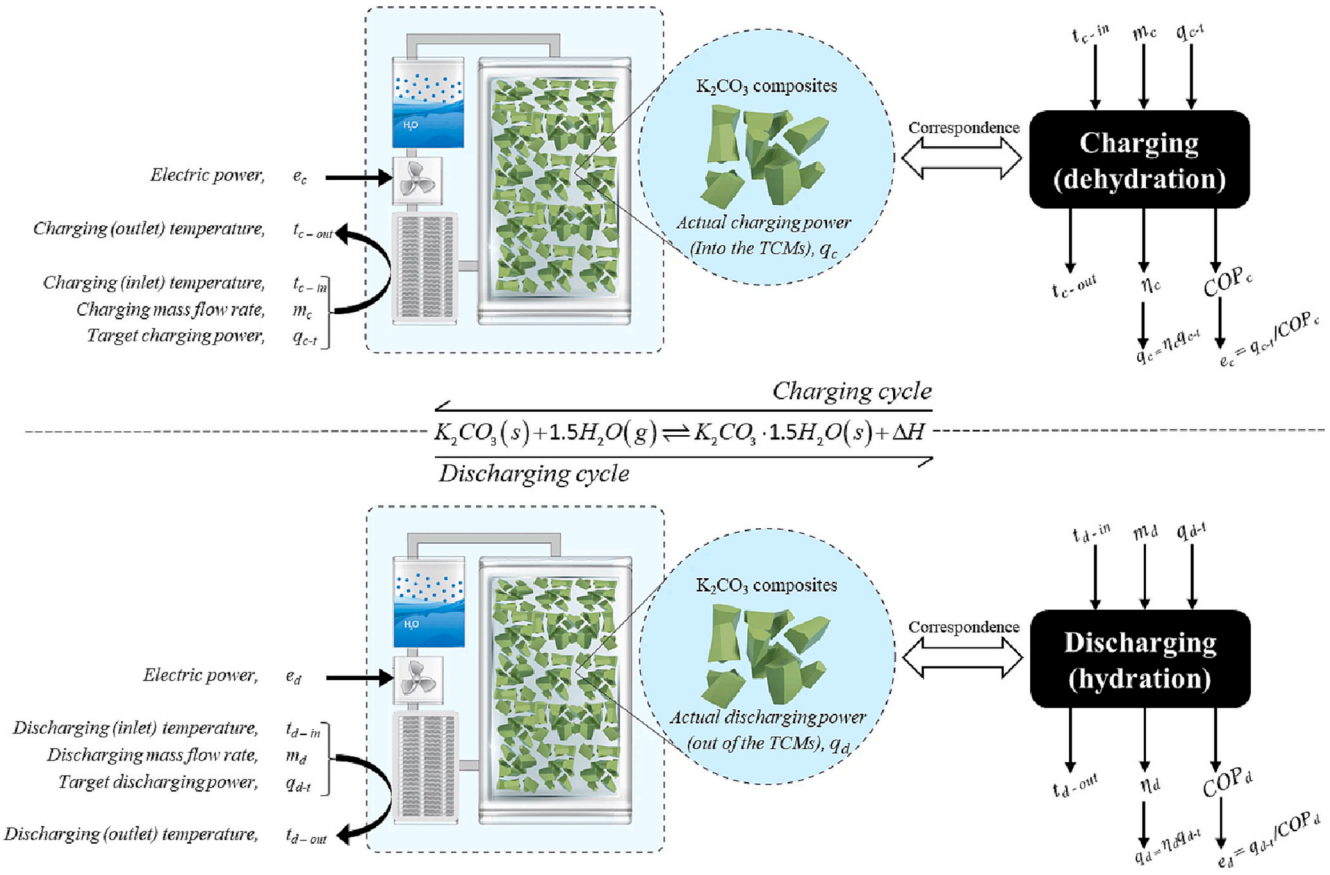

Fig. 3. Schematic diagram of charging/discharging cycles and the corresponding models [45].

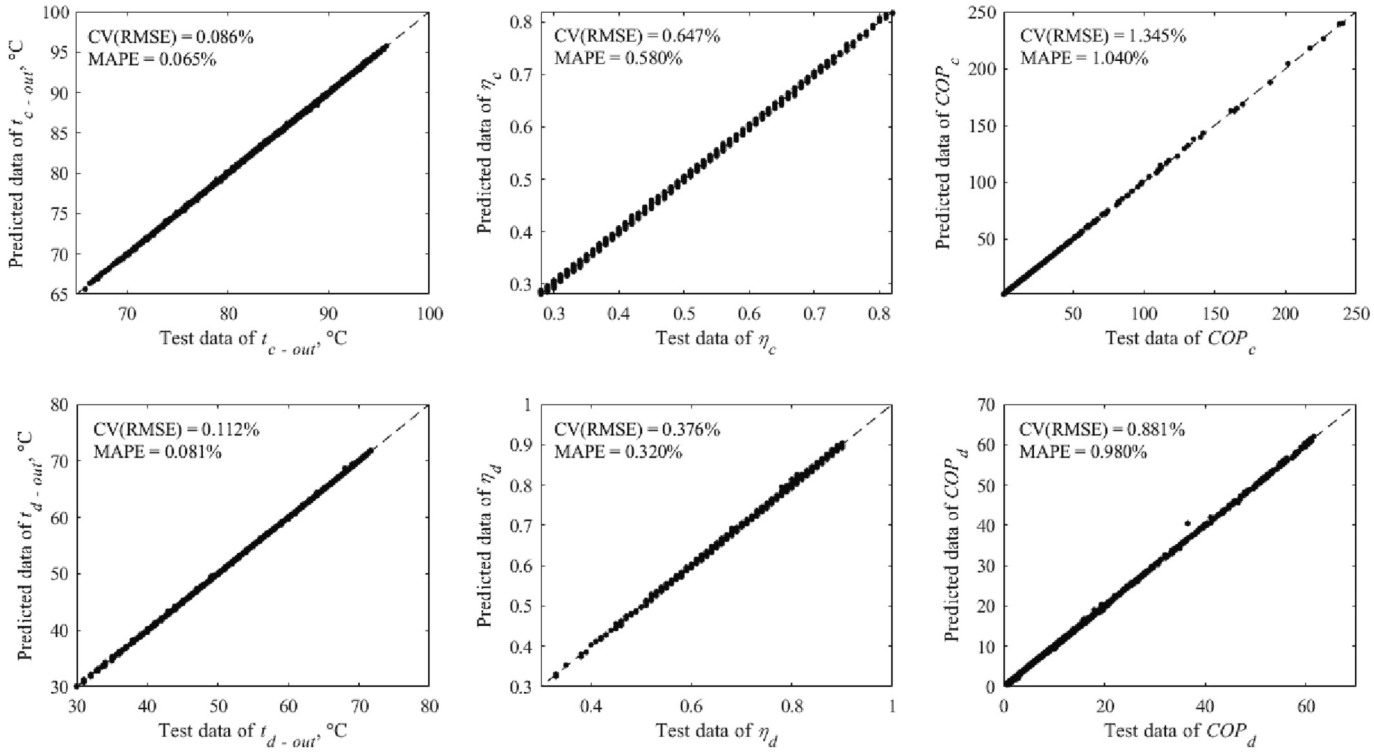

Fig. 4. Test vs predicted data of the output variables of the charging (above) and discharging (below) neural network models.

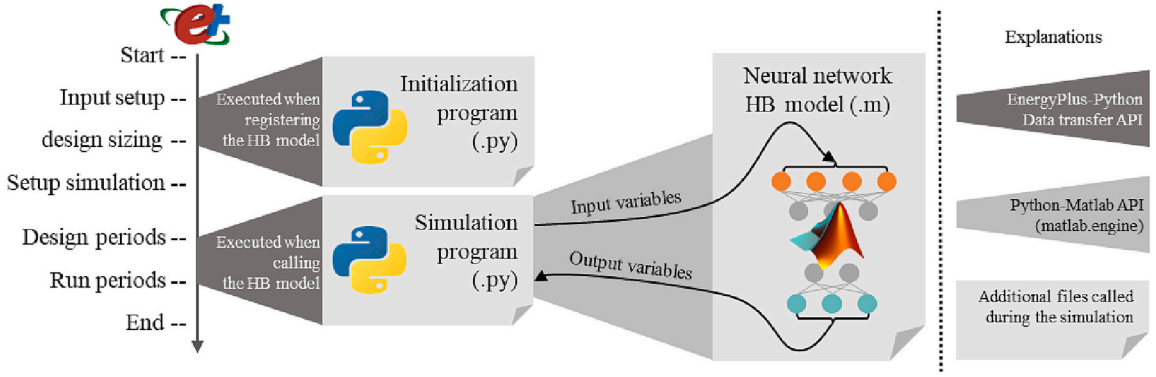

Fig. 5. Execution of additional files for implementing the HB model in EnergyPlus simulation.

the training dataset. Based on the error, the parameters are changed and then fed into the neural network again [46]. The neural network fitting tool in MATLAB is used to train the surrogate model for the charging and discharging processes of the HB. When training the charging model, this study randomly selected 80 % of the data as the training dataset, 10 % as the validation set, and the remaining 10 % as the test set. For the discharging model, in light of the larger data size, this research used 90 % for training and in total 10 % for validation and testing. Furthermore, to choose a proper model complexity, this work considered different layer sizes and training algorithms and compared the accuracy of the trained models. For the charging process, 20 layers and Bayesian Regularization led to the lowest prediction error and avoided under-fitting and over-fitting. For the discharging process, the most proper combination is 15 layers and Levenberg-Marquart.

Fig. 4 presents how the selected models perform on the hold-out test data. The values of the Coefficient of Variation of Root Mean Square Error (CV(RMSE)) and Mean Absolute Percentage Error (MAPE) between the test and predicted data are given on the top-left of each subplot in addition. All the CV(RMSE) values are below 15 %, and all the MAPE values are below 5 %, which indicates an acceptable accuracy according to [47,48]. Meanwhile, both the charging and discharging models can complete the prediction within three milliseconds, which is 20,000 times faster than the physics-based model.

2.2. Part II – HB model implementation and verification

2.2.1. Implementing the HB model in BPS

In order to implement the neural network models in BPS, a simulation engine that allows the embedding of a customized model is needed. For this reason, this method selected the open-source BPS tool EnergyPlus for the whole building energy simulation. It is managed by the National Renewable Energy Laboratory (NREL) and funded by the U.S. Department of Energy [49]. Its recent versions (newer than 9.3) have an application programming interface (API) enabling customized programs to be plugged in [50].

This method used the *PlantComponent: UserDefined* object in EnergyPlus's input file to create a shell for the HB and then connect it with the interface of the HVAC system. Two branches of the user-defined component were used to represent the HB's charging and discharging heat exchangers. The charging branch was defined as demand load mode, which can turn the loop on when it needs a flow. The discharging branch was defined to meet load with a nominal capacity. It can request flow but cannot initiate it. Based on the created shell, this method includes a Python script to define the fundamental energy balance equations and control logic of the HB model. The script has five derived classes from the EnergyPlusPlugin base class. Two of them override the *on_user_defined_component_model* functions to respectively initialize and simulate the charging branch, and two for the discharging branch. The remaining class overrides the *on_end_of_zone_timestep_after_zone_reporting* function to update the state of the HB and report desired output variables. When updating the HB's state, the stored heat inside the materials is calculated by:

$$\frac{dQ_s}{d\tau} = \eta_c q_{c-t} + \frac{q_{d-t}}{\eta_d}; \tag{1}$$

$$q_{c-t} = c_{pc} m_c (t_{c-in} - t_{c-out}); \tag{2}$$

$$q_{d-t} = c_{pd} m_d (t_{d-in} - t_{d-out}). \tag{3}$$

Here, the Q_s (kJ) is the thermal energy stored inside the TCM, and τ (s) is the time. On the other side of the equation, the $q_{c\text{-}t}$ and $q_{d\text{-}t}$ (kW) are the target charging and discharging powers set for the heat battery. The η_c and η_d are the efficiencies of charging and discharging. The c_{pc} and c_{pd} (kJ/kg·K^{-1}) in denote the specific heat capacity of the charging and discharging fluid. The m_c and m_d (kg/s) are the mass flow rates of the charging and discharging fluid. The $t_{c\text{-}in}$ and $t_{d\text{-}in}$ (K) are the charging and discharging fluid temperatures at the inlets of the heat exchangers while The $t_{c\text{-}out}$ and $t_{d\text{-}out}$ (K) are the outlet temperatures.

The electricity consumed by the circulating system is calculated by:

$$\frac{dE}{d\tau} = \frac{q_{c-t}}{COP_c} + \frac{q_{d-t}}{COP_d}. \tag{4}$$

Here, the E (kJ) is the electricity consumed by the HB. The COP_c and COP_d are the coefficients of performance of the charging and discharging processes. Note that the charging and discharging processes cannot happen simultaneously.

Fig. 5 illustrates when the additional files are used in an EnergyPlus simulation run for implementing the HB model. During the initialization process, the initialization program in Python will register basic design parameters (such as the storage capacity, maximum charging or discharging power) of the HB for the following simulation processes. In each simulation timestep of the charging or discharging processes during the design and run periods, the HVAC system models in EnergyPlus will deliver the values of $q_{c\text{-}t}$, $q_{d\text{-}t}$, $t_{c\text{-}in}$, $t_{d\text{-}in}$, m_c, m_d, c_{pc}, c_{pd} to the plugin program in Python. There, the embedded neural network models take these values in and output $t_{c\text{-}out}$, $t_{d\text{-}out}$, η_c, η_d, COP_c, and COP_d. Based on the correspondence shown in Fig. 3, the Python program calculates Q_s and E and reports the required variables back to the running EnergyPlus simulation. The simulation timestep should be defined according to the response time of HB in terms of the time for reaching a stable charging or discharging state.

2.2.2. Verifying the implementation

The implementation of the developed model in EnergyPlus is verified via a test run simulation which will predict the performances of the system and the building. The test run should be designed based on the knowledge of the method user or existing case with data for reference so that the logic between the simulation result and assumptions could be

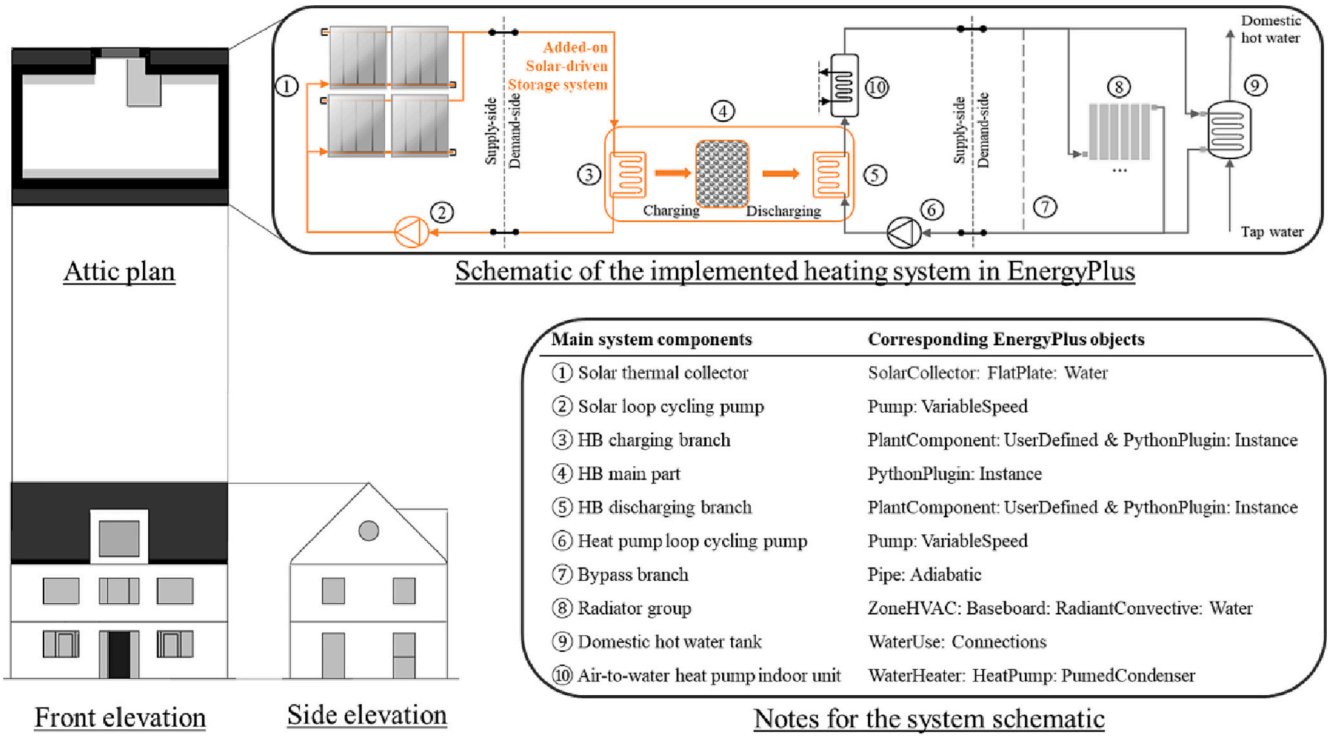

Main system components	Corresponding EnergyPlus objects
① Solar thermal collector	SolarCollector: FlatPlate: Water
② Solar loop cycling pump	Pump: VariableSpeed
③ HB charging branch	PlantComponent: UserDefined & PythonPlugin: Instance
④ HB main part	PythonPlugin: Instance
⑤ HB discharging branch	PlantComponent: UserDefined & PythonPlugin: Instance
⑥ Heat pump loop cycling pump	Pump: VariableSpeed
⑦ Bypass branch	Pipe: Adiabatic
⑧ Radiator group	ZoneHVAC: Baseboard: RadiantConvective: Water
⑨ Domestic hot water tank	WaterUse: Connections
⑩ Air-to-water heat pump indoor unit	WaterHeater: HeatPump: PumedCondenser

Fig. 6. Schematic of the building geometry and heating system configuration models in EnergyPlus.

analyzed. The questions to be checked are, e.g.: Is the state-of-charge fluctuation of the HB in line with the variation of solar heat supply and building heat demand? Can the solar-driven storage system reduce the electricity consumption of the detached house without any apparent sacrifice of indoor thermal comfort? In case of unexpected simulation results from the test run, the possible cause or bug should be analyzed based on the above logic and the simulation workflow. Then, the test run would be re-conducted with an updated assumption or corrected simulation setup.

2.3. Part III – system design optimization

The design optimization of the HB is performed based on a use case. As our previous study defined, a use case consists of the stakeholder, value, strategy, facility, and scenario [27]. The value (key performance indicator) that the stakeholder concerns the most would be the objective and the facility (building property and system configuration) provides the system design option and the boundary condition. When using the HB for consuming onsite solar thermal energy, the reduction of imported electricity is a proper indicator for assessing the value that the system can bring to the homeowner. In addition, common alternatives for the HB such as water tanks can be used as a benchmark for identifying the actual value brought by the HB rather than the solar thermal collectors.

3. Method demonstration: use case description

3.1. Building and heating system configuration

Based on the results of our previous study [27], the following use case was selected: the owner of a detached house wants to use the HB to store the thermal energy collected by the solar collectors and consumes it for its own heat demand in order to reduce imported electricity.

As shown in Fig. 6, the detached house is assumed to have the geometry of the reference building *Woning L vrij* from [39] and matches the insulation level of Dutch houses constructed from 1992 to 2014 in the NTA 8800: 2022 [51]. Its façade, floor, and roof have an R_c value of 2.5 m^2·K/W and its windows have U_w values of 1.8 W/m^2·K. The house has replaced the natural gas boiler with an air-to-water heat pump to meet the *target and ambition for 2030* proposed in the *national climate agreement* [52], and the heat pump is assumed to have a nominal heating capacity of 12 kW and a rated COP of 4.0 (based on the conditions of 7/6 °C DB outdoor air temperature and 30/35 °C inlet/outlet water temperature).

Based on these assumptions and the climate conditions of Eindhoven in 2020 [51], an initial simulation study was conducted; the annual electricity consumption of this building was predicted to be around 9 MWh. According to the *StatLine database* of Statistic Netherlands (also known as CBS) [42], the average gas consumption of a detached house in Eindhoven was 2000 m^3 in 2020, and the average electricity consumption was 4.6 MWh. Assuming that all the domestic gas-fired devices (like gas boilers) are replaced by such electric ones as heat pumps, an annual electricity consumption of 8–10 MWh could be expected for the modeled houses, which covers the predicted value.

As described in the use case, the homeowner wonders whether it is promising to couple the existing heating system with a solar-driven thermochemical storage system (solar collectors and the HB). Therefore, this case study configured a heating system accordingly and set up the model as illustrated in Fig. 6. The solar collector was modeled based on the performance of a 2 m^2 glazed flat plate collector certificated by the Solar Rating & Certification Corporation [52].

The occupancy and heating profiles in this house (in terms of occupant number, lights and appliances, and thermostat) were set to represent two seniors residents as defined in [41], and each occupant was assumed to consume 40 l of hot water every day [53] based on the *Average residential EU (Annex 42)* profile described in [40]. The normal response time of the current HB prototype is around 15 min, so the system timestep of the simulation was defined as 15 min as well.

In order to verify the proposed approach and check the performance of the HB, a test run simulation was first conducted with a default solar collector number of four (8 m^2), a heat battery storage volume of 320 L (93 kWh), and a weather file of Eindhoven [51]. The predicted performances of the system and the building in the test run are checked to

Table 1
Design variants of the solar-driven storage system.

System design variant	Solar collector area, m^2	Storage volume, L
1	8	80
2	16	80
3	8	160
4	16	160
5	8	320
6	16	320
7	8	480
8	16	480
9	8	640
10	16	640
11	8	800
12	16	800
13	8	960
14	16	960

verify the correct implementation of the HB model.

3.2. System design variants

Considering the advantages of sensible heat storage in diurnal charging/discharging cycles, some design variants were also defined to have water tanks with the same storage volumes as indicated in Table 1. The building models with the water tank include similar system connections as the models with the HB and similar operational strategies. The water tank models include heat losses. Two options for solar collectors area (8 to 16 m^2) were considered to investigate the influence of this parameter. In addition to Eindhoven, the climate of Marseille was also taken into account because of its vast solar energy resources. The considered areas of the solar collectors are smaller than the south-facing roof of the detached house, and the selected volumes of the HB are smaller than half the volume of the attic.

The predicted amount of annual heating electricity consumption in all 56 simulation runs are compared in order to reveal the impact of system sizes on the reduction of electricity consumption. The reduction in each case was divided by the area of solar collectors and the storage volume (of the HB or the WT) to locate the optimal storage volume in the whole considered range.

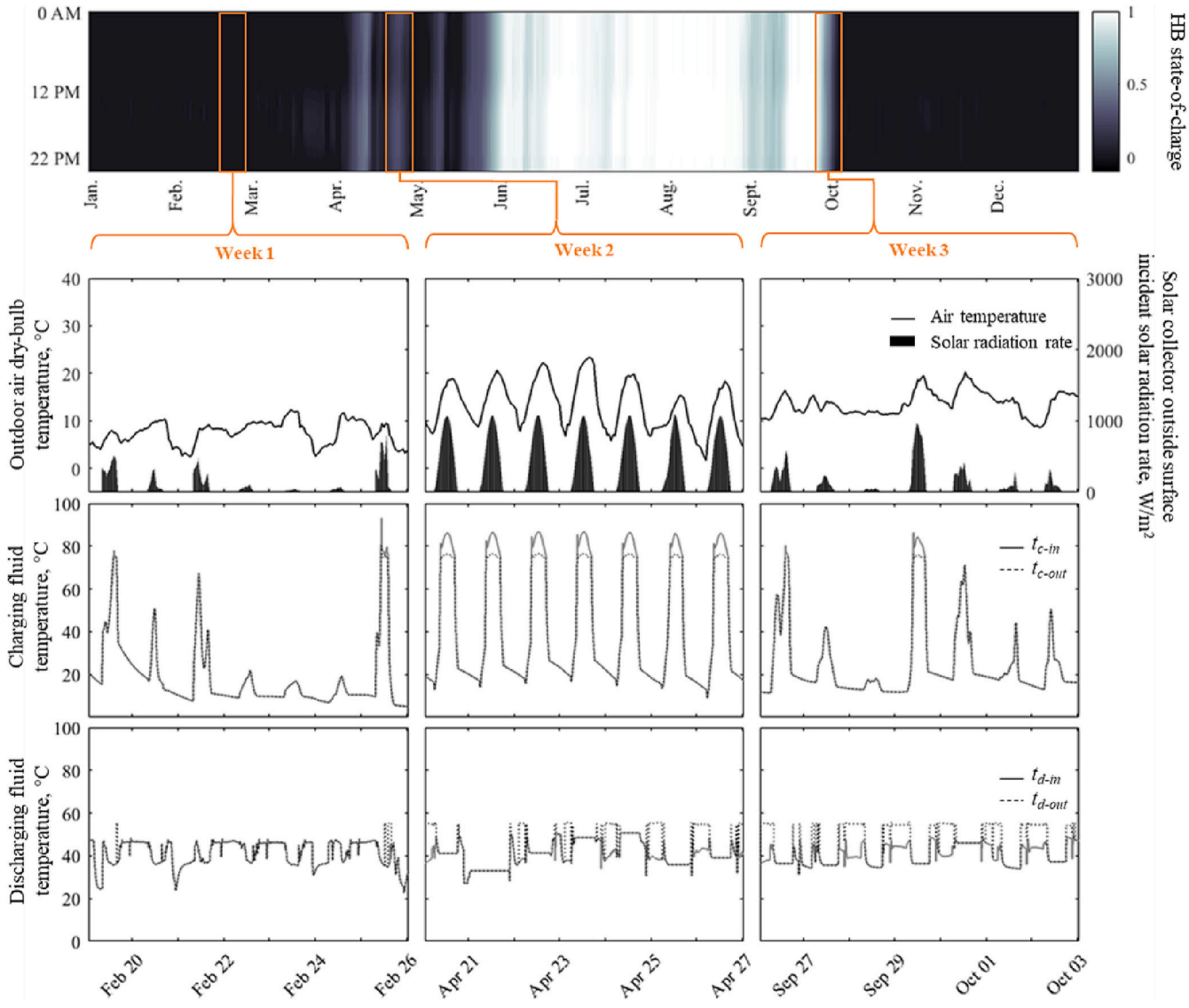

Fig. 7. Predicted year-round state-of-charge fluctuation and three-week charging & discharging processes of the 93 kWh heat battery.

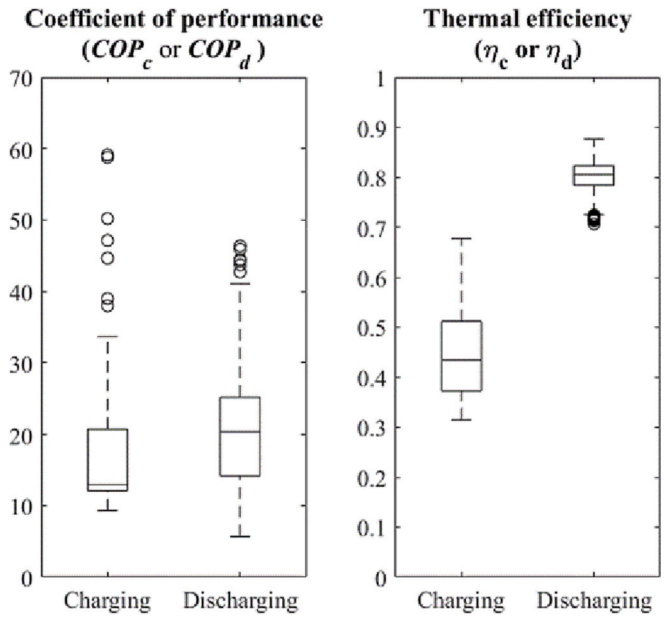

Fig. 8. Predicted values of the HB's charging/discharging COP and thermal efficiency in the simulation year.

4. Method demonstration: result and analysis

4.1. Simulation results for verification of the HB model implementation

4.1.1. Performance of the solar-driven heat battery

The top part of Fig. 7 shows a heatmap with the predicted year-round fluctuation of the HB's state-of-charge. It revealed an obvious seasonal difference in the use of the storage capacity on grounds that the HB was highly occupied from June to September but almost empty during the first and last three months of the simulation year. To further reveal the relations between the weather and the state-of-charge, three typical weeks of the year were selected and the key output variables from the simulation results were visualized as also shown in Fig. 7.

In Week 1 (the last week of February) the weather in Eindhoven was both cold and cloudy as indicated by the curves of the outdoor air dry-bulb temperature and the solar radiation rate. As a consequence, the charging fluid was not heated up sufficiently to transfer the absorbed solar thermal energy to the HB during the first six days, which can be seen from the middle graph for week 1. However, as the weather turned sunny on the last day, some temperature differences also appeared for both the charging and discharging fluid which indicated a cycle of charging-discharging. Week 1 is a typical week when the HB was insufficiently used in terms of both charging and discharging.

In Week 2 (near the end of April) the weather was sunny and warm. Under this weather condition, the HB experienced a stable process of both charging and discharging as shown in the middle and bottom graphs for week 2. The charging process started once the fed fluid became warmer than 75 °C, and it lasted until the temperature fell below this value. With the sufficiently charged HB, the discharging fluid from the demand side could be heated up to its setpoint (around 55 °C). Week 2 is a typical week when the HB could reach a proper balance between charging and discharging.

Week 3 (last days of September and first days of October) show that after being charged for a whole summer, the HB was almost full at the beginning of this week. Therefore, although it was not very sunny except on the fourth day, a stable discharging period can still be witnessed from those temperature increases of the discharging fluid in the bottom graph for week 3. This week is a typical week when the HB released the summer heat to meet the demand in the transition season.

The results in these three weeks reveal how much impact the weather conditions have on the charging performance of the HB in this system. Continuous sunny and warm weather can lead to hotter charging fluid and thus enable stable and effective charging cycles. Different from charging, the discharging processes of the HB presented a more steady mode in this system, as the HB can meet its setpoint if only there is enough heat stored inside it. This difference becomes more evident from the perspective of the whole simulation year. Furthermore, the season difference in the HB's state-of-charge also indicates a possible impact caused by the area of the collectors and the storage capacity of the HB.

The left boxplot of Fig. 8 tells both the predicted ranges of the charging and discharging COP values of the HB and their overall difference. In this simulation year, the median charging COP was predicted to be around 12 while the median discharging COP was about 21. A similar difference also exists between the predicted thermal efficiency of charging and discharging, as the discharging efficiency distributed around 80 % while the charging one was around 45 %.

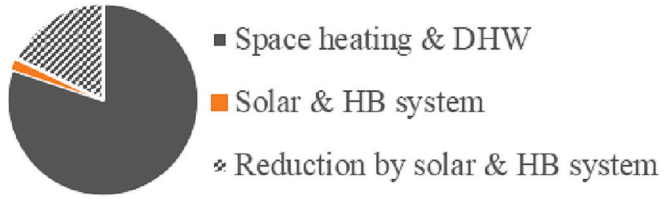

Fig. 9. The annual reduction of heating electricity consumption in the detached house by the 8 m^2 solar thermal collectors and 93 kWh heat battery.

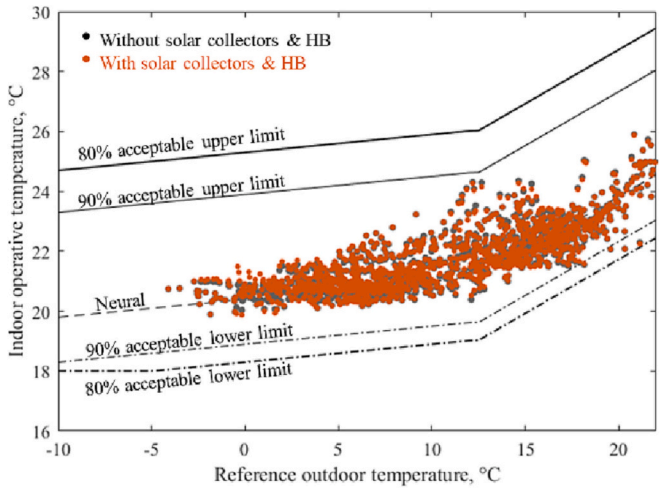

Fig. 10. Living room operative temperature during occupied hours with and without 8 m^2 solar thermal collectors and 93 kWh heat battery.

4.1.2. Performance of the building

With this default heating system configuration (8 m^2 solar thermal collectors and 93 kWh heat battery), the detached house imported approximately 5 MWh from the local electricity grid for space heating and domestic hot water. For the house without any solar collector or HB, the electricity consumed by the same sector was around 6 MWh, which indicated a 16 % reduction by the integration of the solar-driven storage system as shown in Fig. 9. Compared with this reduction, the additional electricity consumed by the solar loop pump and the heat battery is not significant. The possible prediction error from the neural network HB model could influence this result, but even the highest MAPE (1 % for the discharging COP) would not obviously impact the scales of the reduction part and the solar & HB part in Fig. 9.

Besides energy performance, it is also crucial for the homeowner how the integration of the HB and solar collector could shape the indoor thermal comfort of this building. So the operative temperature in the

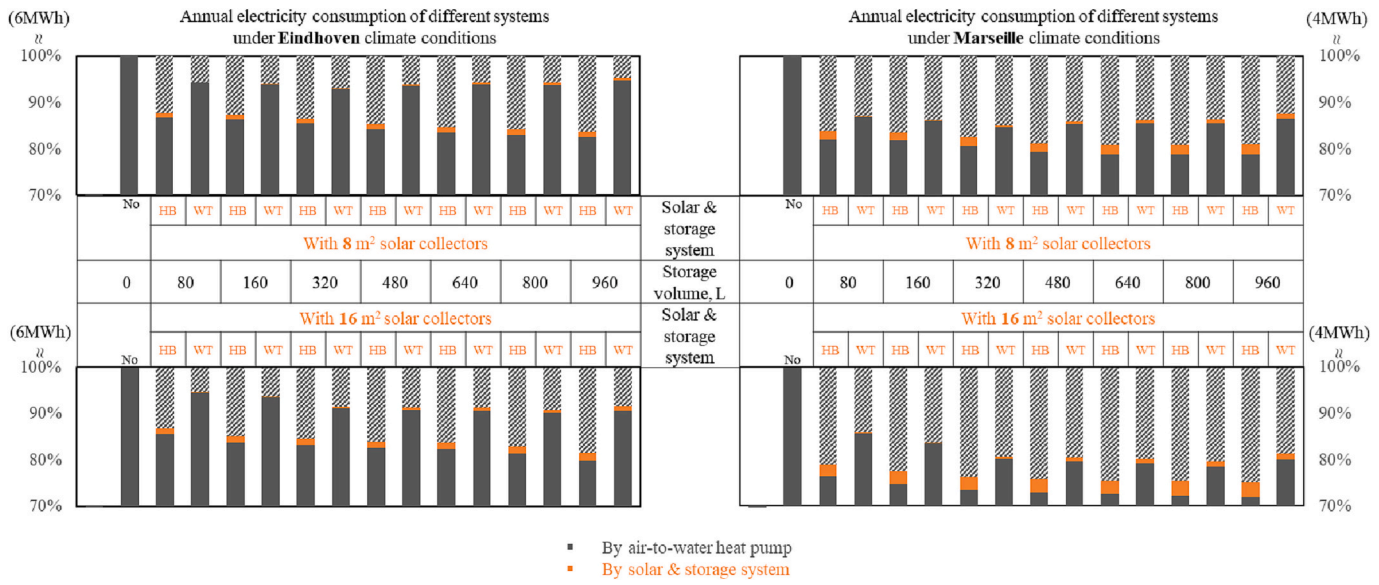

Fig. 11. Annual electricity consumptions of different heating system variants in the detached house under Eindhoven and Marseille climate conditions (HB = heat battery while WT = water tank).

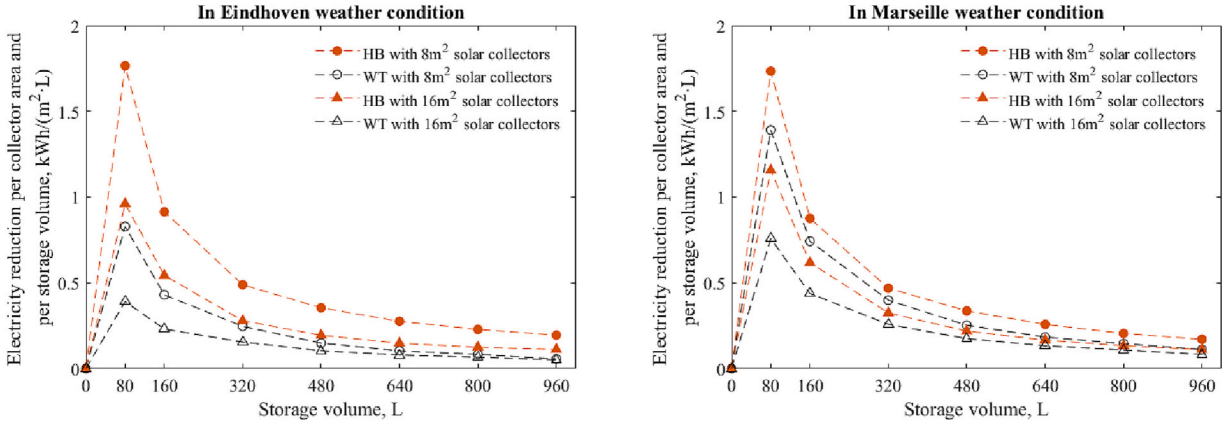

Fig. 12. Relationships between storage volume and the electricity reduction per area solar collector and per storage volume in two weather conditions.

living room was also checked during the occupied hours in the simulation year based on the acceptable regions proposed by [54]. As shown in Fig. 10, the integration of the solar & storage system did not change the thermal comfort in the living room when it was occupied. The results above indicate the correct implementation of the HB model in EnergyPlus.

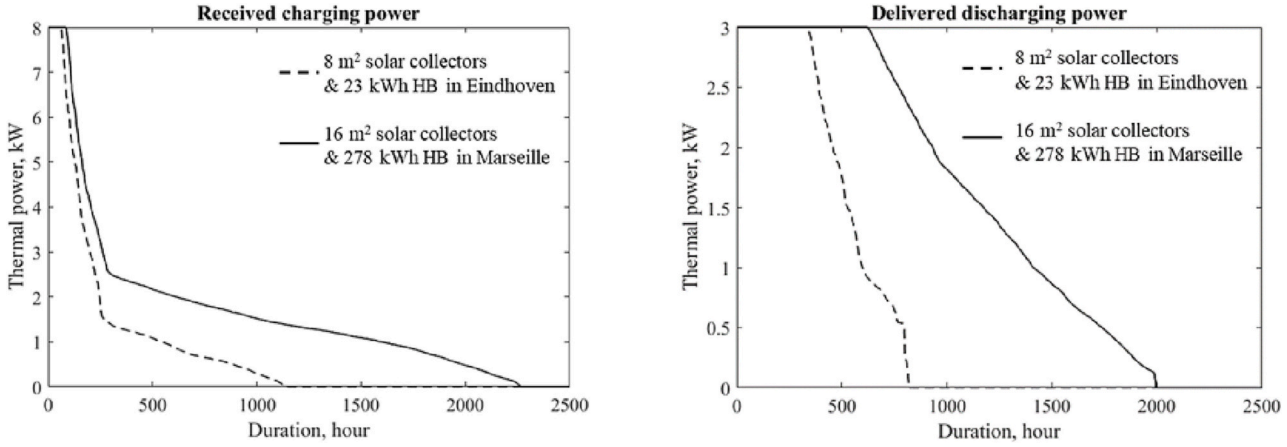

Fig. 13. Duration curves of the charging/discharging powers received/delivered by the HBs in two extreme cases.

4.2. The optimal design

The results of 56 simulations (28 system variants under two different climate conditions) for design optimization are shown in Fig. 11. A larger storage capacity of the HB leads to lower electricity consumption by the heat pump, but this effect is not significant. For instance, in the top-right bar chart, the largest storage capacity is almost 12 times the size of the smallest one but only brings around a 5 % further reduction. However, water tanks show a different trend. The increase in storage volumes results in both more digested solar thermal energy and more heat loss, especially from the larger area of tank surfaces. The increase in solar collector areas also leads to more digested solar thermal energy. This is obvious in the results under Marseille climate where around 10 % further reduction was provided by the increase of the collector area. But as the solar & storage system was turned on more frequently, its own electricity consumption also increased. The climate makes a difference in the percentage of reduction by the solar & HB systems, as the values for Eindhoven were around 10–15 % and those for Marseille ranged from 20 to 25 %. In general, a small-scale HB already shows a promising potential for digesting solar thermal energy, while the potential of the HB is also larger than the water tank in every investigated case.

Dividing the reduction of annual electricity consumption in all 56 cases by the area of solar collectors and the storage volume, this study got eight trend lines for analyzing the effect of increasing storage volume as shown in Fig. 12. In all 56 cases, the storage volume increase from 0 to 80 l brings a higher electricity reduction per area collector per volume than further ones, which indicates that the optimal storage volume in the considered range (80–960 l) would be around 80 l but below 160 l. The considered two climates do not make an obvious difference in this.

Although the maximum charging and discharging powers are set as the same in all system variants, the usage of them is also valuable for the further development of the HB. Two extreme cases were selected from all the simulation runs and the duration curves of the charging/discharging powers received/delivered by these two HBs were visualized in Fig. 13.

Because the HBs were mostly full during the summer when the charging power went up, the received charging powers of both the 23 kWh and 278 kWh HBs remained below half of the allowed maximum value (8 kW) for a rather long duration. This signifies a possible space for adjusting the charging power to further compact the small-scale HB and improve the efficiency of using its capability. But the curves of discharging power showed different shapes. Each range of discharging power values lasted for a notable time for both HBs here, which indicated a reasonable and efficient usage of the designed capacity.

5. Conclusion

This article proposed a novel simulation-based design optimization method for solar-driven thermochemical heat storage systems in building applications. The method was demonstrated to assess the performance of a state-of-the-art closed-loop thermochemical heat storage system in a detached house and identified the optimal design of the system in two climates. To achieve this, a computationally cheap surrogate model is implemented in the Building Energy Simulation program EnergyPlus by using its API functionality. The model was validated by calculating the CV(RMSE) (below 15 %) and MAPE (below 5 %), and the implementation was verified by a test simulation run. The simulation results show that the HB has the potential for reducing around 0.7–1 MWh of the electricity consumption for space heating and hot tap water by digesting the heat transferred from solar thermal collectors in the studied case. The reduction by each considered size of the HB was higher than the same-storage-volume water tank, and did not cause any sacrifice in the indoor thermal comfort.

The increase in storage volume from 0 to 80 l brings a higher reduction of electricity consumption per collector area per storage volume compared to 80 l and above, which implies that the optimal storage volume of the HB is around 80 l and below 160 l in the considered range. The result also suggests that it is not worthwhile to increase the storage volume for achieving seasonal storage in light of the limited space for both the heat battery and solar collectors in a detached house, especially when compared with the specific benefit of water tanks with the same storage volume. The received charging power of the HB did not reach its maximum limit for more than 95 % of the duration in considered cases, which indicates a possible space for compacting the charging unit of the system. All these results suggest that a small-scale HB could be more practical than a large-scale one in this type of daily-storage use case because of the efficient usage of both the storage capacity and charging/discharging powers.

The developed methodology can also be used for investigating other use cases of the HB. For example, the HB can also be used for shifting the peak load on the local grid (heat and electricity), exploiting dynamic energy prices, or for using waste heat in the built environment. In addition to a detached house, the HB can also be deployed in other types of residential buildings, office buildings, as well as a district. The investigation of these use cases remains the direction of future work.

CRediT authorship contribution statement

Shuwei Wang: Conceptualization, Investigation, Methodology, Writing – original draft, Writing – review & editing. **Pieter-Jan Hoes:** Conceptualization, Supervision, Writing – review & editing. **Jan L.M. Hensen:** Conceptualization, Supervision, Writing – review & editing. **Olaf C.G. Adan:** Supervision, Writing – review & editing. **Pim A.J. Donkers:** Data curation, Resources.

Declaration of competing interest

The authors declare that they have no known competing financial interests or personal relationships that could have appeared to influence the work reported in this paper.

Data availability

Data will be made available on request.

Acknowledgment

This research has been supported by project 9.4: development of closed-loop TCM system, which is part of the ‘Integrale Energietransitie Bestaande Bouw’ (IEBB). The IEBB project was initiated by the Building and Technology Innovation Centre (BTIC) and is funded by Rijksdienst voor Ondernemend (RVO) Nederland.

References

[1] IEA, Transition to Sustainable Buildings: Paris, 2013, https://doi.org/10.1787/9789264202955-en.
[2] Eurostat, Share of Renewable Energy in Gross Final Energy Consumption. http://epp.eurostat.ec.europa.eu/tgm/table.do?tab=table&plugin=1&language=en&pcode=t2020_31, 2022 (accessed July 15, 2022).
[3] Q. Chen, Z. Kuang, X. Liu, T. Zhang, Energy storage to solve the diurnal, weekly, and seasonal mismatch and achieve zero-carbon electricity consumption in buildings, Appl. Energy 312 (2022), 118744, https://doi.org/10.1016/J.APENERGY.2022.118744.
[4] L. Miró, J. Gasia, L.F. Cabeza, Thermal energy storage (TES) for industrial waste heat (IWH) recovery: a review, Appl. Energy 179 (2016) 284–301, https://doi.org/10.1016/J.APENERGY.2016.06.147.
[5] M. Babaei, E. Azizi, M.T. Beheshti, M. Hadian, Data-driven load management of stand-alone residential buildings including renewable resources, energy storage system, and electric vehicle, J. Energy Storage 28 (2020), 101221, https://doi.org/10.1016/J.EST.2020.101221.
[6] Z. Mohammadi, P.J. Hoes, J.L.M. Hensen, Simulation-based design optimization of houses with low grid dependency, Renew. Energy 157 (2020) 1185–1202, https://doi.org/10.1016/j.renene.2020.04.157.
[7] Y. Li, F. Qian, W. Gao, H. Fukuda, Y. Wang, Techno-economic performance of battery energy storage system in an energy sharing community, J. Energy Storage 50 (2022), 104247, https://doi.org/10.1016/J.EST.2022.104247.

[8] X. Pan, Y. Xiang, M. Gao, J. Fan, S. Furbo, D. Wang, et al., Long-term thermal performance analysis of a large-scale water pit thermal energy storage, J. Energy Storage 52 (2022), 105001, https://doi.org/10.1016/J.EST.2022.105001.

[9] T.P. Gaonwe, P.A. Hohne, K. Kusakana, Optimal energy management of a solar-assisted heat pump water heating system with a storage system, J. Energy Storage 56 (2022), 105885, https://doi.org/10.1016/J.EST.2022.105885.

[10] X. Qiao, X. Kong, M. Fan, Phase change material applied in solar heating for buildings: a review, J. Energy Storage 55 (2022), 105826, https://doi.org/10.1016/J.EST.2022.105826.

[11] A.M. Nair, C. Wilson, M.J. Huang, P. Griffiths, N. Hewitt, Phase change materials in building integrated space heating and domestic hot water applications: a review, J. Energy Storage 54 (2022), 105227, https://doi.org/10.1016/J.EST.2022.105227.

[12] G. Reynders, T. Nuytten, D. Saelens, Potential of structural thermal mass for demand-side management in dwellings, Build. Environ. 64 (2013) 187–199, https://doi.org/10.1016/J.BUILDENV.2013.03.010.

[13] J. Lizana, R. Chacartegui, A. Barrios-Padura, J.M. Valverde, Advances in thermal energy storage materials and their applications towards zero energy buildings: a critical review, Appl. Energy 203 (2017) 219–239, https://doi.org/10.1016/j.apenergy.2017.06.008.

[14] R.J. Clark, A. Mehrabadi, M. Farid, State of the art on salt hydrate thermochemical energy storage systems for use in building applications, J. Energy Storage 27 (2020), 101145, https://doi.org/10.1016/J.EST.2019.101145.

[15] A. Odukomaiya, J. Woods, N. James, S. Kaur, K.R. Gluesenkamp, N. Kumar, et al., Addressing energy storage needs at lower cost via on-site thermal energy storage in buildings †, Energy Environ. Sci. 14 (2021) 5315, https://doi.org/10.1039/d1ee01992a.

[16] K. Kant, R. Pitchumani, Advances and opportunities in thermochemical heat storage systems for buildings applications, Appl. Energy 321 (2022), 119299, https://doi.org/10.1016/J.APENERGY.2022.119299.

[17] D. Vérez, E. Borri, G. Zsembinszki, L.F. Cabeza, Thermal energy storage co-benefits in building applications transferred from a renewable energy perspective, J. Energy Storage 58 (2023), 106344, https://doi.org/10.1016/J.EST.2022.106344.

[18] W. Li, X. Luo, P. Yang, Q. Wang, M. Zeng, C.N. Markides, Solar-thermal energy conversion prediction of building envelope using thermochemical sorbent based on established reaction kinetics, Energy Convers. Manag. 252 (2022), 115117, https://doi.org/10.1016/J.ENCONMAN.2021.115117.

[19] K. Thinsurat, H. Bao, Z. Ma, A.P. Roskilly, Performance study of solar photovoltaic-thermal collector for domestic hot water use and thermochemical sorption seasonal storage, Energy Convers. Manag. 180 (2019) 1068–1084, https://doi.org/10.1016/J.ENCONMAN.2018.11.049.

[20] E. Borri, G. Zsembinszki, L.F. Cabeza, Recent developments of thermal energy storage applications in the built environment: a bibliometric analysis and systematic review, Appl. Therm. Eng. 189 (2021), 116666, https://doi.org/10.1016/j.applthermaleng.2021.116666.

[21] P.A.J. Donkers, L.C. Sögütoglu, H.P. Huinink, H.R. Fischer, O.C.G. Adan, A review of salt hydrates for seasonal heat storage in domestic applications, Appl. Energy 199 (2017) 45–68, https://doi.org/10.1016/j.apenergy.2017.04.080.

[22] J. Houben, L. Sögütoglu, P. Donkers, H. Huinink, O. Adan, K2CO3 in closed heat storage systems, Renew. Energy 166 (2020) 35–44, https://doi.org/10.1016/j.renene.2020.11.119.

[23] K. Kant, R. Pitchumani, Analysis of a novel constructal fin tree embedded thermochemical energy storage for buildings applications, Energy Convers. Manag. 258 (2022), 115542, https://doi.org/10.1016/J.ENCONMAN.2022.115542.

[24] N. Yu, R.Z. Wang, L.W. Wang, Sorption thermal storage for solar energy, Prog. Energy Combust. Sci. 39 (2013) 489–514, https://doi.org/10.1016/j.pecs.2013.05.004.

[25] J.H. Davidson, J. Quinnell, J. Burch, H.A. Zondag, R. de Boer, C. Finck, et al., Development of Space Heating and Domestic Hot Water Systems with Compact Thermal Energy Storage, 2013.

[26] H. Bao, Z. Ma, Thermochemical energy storage, in: Storing Energy: With Special Reference to Renewable Energy Sources, 2022, pp. 651–683, https://doi.org/10.1016/B978-0-12-824510-1.00028-3.

[27] S. Wang, P. Hoes, J.L.M. Hensen, O.C.G. Adan, P.A.J. Donkers, Identifying promising use cases for a novel heat battery in Dutch residential buildings, TU Delft OPEN (2022) 1–8, https://doi.org/10.34641/clima.2022.165.

[28] S.O. Weber, M. Oei, M. Linder, M. Böhm, P. Leistner, O. Sawodny, Model predictive approaches for cost-efficient building climate control with seasonal energy storage, Energy Build 270 (2022), 112285, https://doi.org/10.1016/J.ENBUILD.2022.112285.

[29] K. Thinsurat, H. Bao, Z. Ma, A.P. Roskilly, Performance study of solar photovoltaic-thermal collector for domestic hot water use and thermochemical sorption seasonal storage, Energy Convers. Manag. 180 (2019) 1068–1084, https://doi.org/10.1016/J.ENCONMAN.2018.11.049.

[30] G. Zisopoulos, A. Nesiadis, K. Atsonios, N. Nikolopoulos, D. Stitou, A. Coca-Ortegón, Conceptual design and dynamic simulation of an integrated solar driven thermal system with thermochemical energy storage for heating and cooling, J. Energy Storage 41 (2021), 102870, https://doi.org/10.1016/J.EST.2021.102870.

[31] J.L.M. Hensen, R.C.G.M. Loonen, M. Archontiki, M. Kanellis, Using building simulation for moving innovations across the "Valley of Death.", REHVA J. 52 (2015) 58–62.

[32] J.L.M. Hensen, R. Lamberts, Building Performance Simulation for Design and Operation 9780203891612, 2012, https://doi.org/10.4324/9780203891612.

[33] Q. Chen, Y. Zhang, Y. Ding, Wettability of molten sodium sulfate salt on nanoscale calcium oxide surface in high-temperature thermochemical energy storage, Appl. Surf. Sci. 505 (2020), 144550, https://doi.org/10.1016/j.apsusc.2019.144550.

[34] S. Lan, Grain-Scale Analysis of Thermochemical Heat Storage Materials, Technische Universiteit Eindhoven, 2016.

[35] Z. Pan, C. Zhao, Prediction of the effective thermal conductivity of packed bed with micro-particles for thermochemical heat storage, Sci. Bull. (Beijing) 62 (2017) 256–265, https://doi.org/10.1016/J.SCIB.2016.12.009.

[36] Z.H. Pan, C.Y. Zhao, Gas–solid thermochemical heat storage reactors for high-temperature applications, Energy 130 (2017) 155–173, https://doi.org/10.1016/j.energy.2017.04.102.

[37] A.J.H. Frijns, C.C.M. Rindt, S.v. Gaastra-Nedea, Modeling Thermochemical Reactions in Thermal Energy Storage Systems. LTD, 2020, https://doi.org/10.1016/B978-0-12-819885-8.00017-6.

[38] A. Crespo, C. Fernández, D. Vérez, J. Tarragona, E. Borri, A. Frazzica, et al., Thermal performance assessment and control optimization of a solar-driven seasonal sorption storage system for residential application, Energy 263 (2023), 125382, https://doi.org/10.1016/J.ENERGY.2022.125382.

[39] Referentie gebouwen BENG (Bijna EnergieNeutrale Gebouwen). 2017.

[40] E. Fuentes, L. Arce, J. Salom, A review of domestic hot water consumption profiles for application in systems and buildings energy performance analysis, Renew. Sust. Energ. Rev. 81 (2018) 1530–1547, https://doi.org/10.1016/j.rser.2017.05.229.

[41] O. Guerra-Santin, S. Silvester, Development of Dutch occupancy and heating profiles for building simulation, Build. Res. Inf. 45 (2017) 396–413, https://doi.org/10.1080/09613218.2016.1160563.

[42] CBS. StatLine - Energy Consumption in Private Homes; Housing Type and Regions 2021. https://opendata.cbs.nl/statline/#/CBS/nl/dataset/81528NED/table?ts=1656668035543 (accessed July 1, 2022).

[43] Cellcius BV. Cellcius Homepage n.d. https://cellcius.com/en/ (accessed March 8, 2023).

[44] N. Mazur, H. Huinink, H. Fischer, P. Donkers, O. Adan, Accelerating the reaction kinetics of K2CO3 through the addition of CsF in the view of thermochemical heat storage, Sol. Energy 242 (2022) 256–266, https://doi.org/10.1016/J.SOLENER.2022.07.023.

[45] Heat-Insyde. Heat Battery Introduction n.d. https://www.heat-insyde.eu/project/technologies/ (accessed October 19, 2021).

[46] D. Ayon, Machine learning algorithms : a review, Int. J. Comput. Sci. Inform. Technol. 7 (2016) 1174–1179, https://doi.org/10.21275/ART20203995.

[47] G.R. Ruiz, C.F. Bandera, Validation of calibrated energy models: common errors, Energies (Basel) (2017) 10, https://doi.org/10.3390/en10101587.

[48] D.A. Swanson, On the relationship among values of the same summary measure of error when it is used across multiple characteristics at the same point in time: an examination of MALPE and MAPE, Rev. Econ. Finan. 5 (2015) 1–14 (ISSN(p) 1923-7529, ISSN(e) 1923-8401).

[49] EnergyPlus homepage n.d. https://energyplus.net/ (accessed June 20, 2022).

[50] National Renewable Energy Laboratory for the United States Department of Energy. EnergyPlus Python API 0.1 Documentation n.d. https://nrel.github.io/EnergyPlus/api/python/ (accessed March 8, 2023).

[51] Koninklijk Nederlands Meteorologisch Instituut, Hourly Data for the Weather in the Netherlands. https://www.knmi.nl/nederland-nu/klimatologie/uurgegevens, 2022.

[52] SRCC, OG-100 Solar Thermal Collector Certification, 2020.

[53] NEN, Nederlandse Technische Afspraak NTA 8800:2022, 2021.

[54] L. Peeters, R. de Dear, J. Hensen, D'haeseleer W., Thermal comfort in residential buildings: comfort values and scales for building energy simulation, Appl. Energy 86 (2009) 772–780, https://doi.org/10.1016/j.apenergy.2008.07.011.